Int. J. Solids Structures, 1965, Vol. 1, pp. 385 to 406. Pergamon Press Ltd. Printed in Great Britain

THE DYNAMIC STABILITY OF A SIMPLIFIED FOUR-WHEELED RAILWAY VEHICLE HAVING PROFILED WHEELS

A. H. WICKENS
British Rail Research Department, Derby

Abstract—The dynamic instability of a four-wheeled railway vehicle, due to the combined action of the creep forces acting between the wheels and the rails and the conicity of the wheels, is investigated in the case where the vehicle body is attached to the wheels by means of an elastic suspension. The suspension is assumed to have negligible stiffness in the longitudinal direction, and the wheel treads are profiled instead of being purely conical. It is shown that there are two possible types of instability; the wheelset instability which occurs at high speeds and which involves mainly wheelset motion and the body instability which occurs at low speeds and involves large displacements of the body. The effect of the restoring force which arises from the lateral component of the variation of the normal reaction between wheel and rail with lateral displacement is shown to have an important effect on stability, and it is indicated how this effect can be exploited in conjunction with suspension damping in the proper design of a railway vehicle for stable running at high speeds.

NOTATION

a_i	amplitude of displacement in ith freedom
C	moment of inertia in yaw of wheelset
C'	moment of inertia in yaw of body
f, f'	longitudinal and lateral creep coefficients
g	hysteretic loss factor
G	$= \varepsilon_2 g/\mu'\alpha$
hl	length defined in Fig. 1
j	$= C/ml^2$
k_1, k_2	suspension elastic stiffness coefficients in longitudinal and lateral directions
K	$= (2\mu + 2\mu' j)/\rho\mu$
l	length defined in Fig. 1
m	mass of wheelset
m'	mass of body
p_i	coefficient in characteristic equation
q_s	generalized co-ordinate
Q_s	generalized force
r_0	wheel tread circle radius, wheelset in central position
R	radius of curvature of wheel tread
R'	radius of curvature of rail head
s	$= \frac{l}{V_0}\frac{\mathrm{d}}{\mathrm{d}t}$
t	time
v	$= V/V_0$
v_c	non-dimensional critical speed
V	forward speed of vehicle
V_0	reference speed
W	axle-load
α	$= \lambda l/r_0$
δ_0	angle between contact plane and horizontal, wheelset in central position
ε	rate of change of the angle between contact plane and horizontal with lateral displacement, divided by l

$\varepsilon_1, \varepsilon_2, \varepsilon_2$	non-dimensional stiffness coefficients
θ	phase angle
λ	effective conicity
λ_i	$= \eta_i + i\nu_i$, root of characteristic equation
Λ	$= v/v$
μ, μ'	non-dimensional creep coefficients
ν	$= \omega l/V_0$
ρ	$= m'/m$
σ	$= C'/ml^2$
ψ_i	non-dimensional generalized co-ordinate
ω	circular frequency
Ω	$= v\sqrt{(\rho/2\varepsilon_2)}$

INTRODUCTION

THE dynamic instability of railway vehicles is due to the non-conservative forces acting between the wheels and the rails, which arise from the phenomenon of creep. In [1] a linearized stability analysis of a single bogie or wheelset (a wheelset consisting of two wheels mounted on a rigid common axle) having profiled wheels was considered. It was assumed there that the vehicle body did not participate in the motion at the critical speed, and so it is the purpose of the present paper to present an analysis including the motion of the body. It is found that a complete vehicle may experience two forms of instability, the wheelset instability which is discussed in [1] and which occurs at high speeds and the body instability which involves large motions of the vehicle body and which usually occurs at much lower speeds than the wheelset instability.

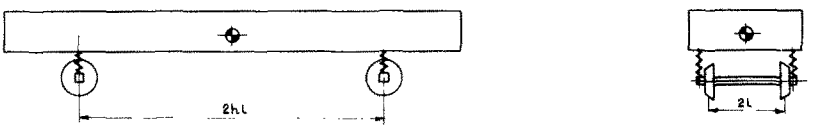

FIG. 1. Arrangement of railway vehicle.

Much of the earlier work on the stability of railway vehicles [1] was concerned with locomotives, and little work has been carried out on vehicles in which the stability is dominated by the action of the suspension. Matsudeira [2] and Kovalev [3] have considered the effects of lateral and longitudinal suspension flexibility on the stability of four-wheeled railway vehicles, but neglected the gravitational stiffness effect. This effect is the lateral restoring force which arises from the variation of the normal reaction between wheel and rail with lateral displacement, and while it is negligible in magnitude for conical wheels, it can be very large for profiled wheels. It is shown below that this effect is very important, and can be exploited in the design of a railway vehicle for running at high speeds.

As it is desirable to consider as simple a system as possible, the theory developed here assumes a vehicle possessing two wheelsets (Fig. 1) which is moving along the track at constant speed. Each wheelset is connected to the vehicle body, which is assumed to be rigid, by means of a suspension which possesses stiffness in the lateral direction only. The neglect of longitudinal suspension stiffness not only simplifies the stability analysis considerably, but it can be shown that under certain conditions longitudinal stiffness has no effect on stability.

EQUATIONS OF MOTION

Neglecting rolling motions of the vehicle body, the motions which are antisymmetric with respect to the longitudinal plane of symmetry can be described in terms of six generalized co-ordinates. The analysis will be facilitated if the following co-ordinates (Fig. 2) are chosen:

q_1 equal and opposite lateral displacements of the wheelsets
q_2 equal and opposite yaw displacements of the wheelsets
q_3 yaw of the body about the body centre of mass
q_4 equal lateral displacements of the wheelsets
q_5 equal yaw displacements of the wheelsets
q_6 lateral displacement of the body.

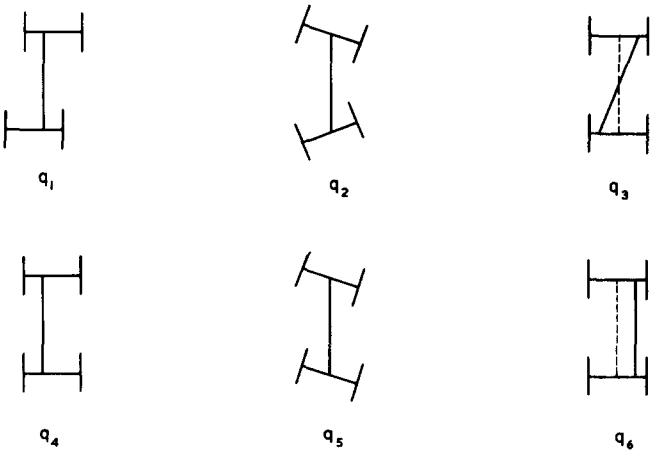

FIG. 2. Motions associated with generalized co-ordinates q_s.

In the absence of suspension damping, the equations of motion of the vehicle are

$$\begin{gathered} m\ddot{q}_1+2k_2(q_1-hlq_3)=Q_1, \qquad C\ddot{q}_2=Q_2, \\ \tfrac{1}{2}C'\ddot{q}_3+2k_2hl(hlq_3-q_1)=0, \qquad m\ddot{q}_4+2k_2(q_4-q_6)=Q_4, \\ C\ddot{q}_5=Q_5, \qquad \tfrac{1}{2}m'\ddot{q}_6+2k_2(q_6-q_4)=0, \end{gathered} \tag{1}$$

where m, m' are the masses of the wheelset and body respectively, C, C' are the moments of inertia in yaw of wheelset and body respectively, k_2 is the lateral suspension stiffness, $2hl$ is the wheelbase and Q_1, Q_2, Q_4 and Q_5 represent the forces applied by the rails to the wheels, expressions for which have been derived in [1], and are

$$Q_1=\frac{-2f'\dot{q}_1}{V}+2f'q_2-W\varepsilon\frac{q_1}{l}, \qquad Q_2=\frac{-2fl^2}{V}\dot{q}_2-\frac{2f\lambda l}{r_0}q_1. \tag{2}$$

Similar expressions exist for Q_4 and Q_5. In equations (2), V is vehicle speed, $2l$ is the distance between contact points on the wheels, r_0 is the radius of the tread circle of the wheels when in the central position, f and f' are the longitudinal and lateral creep coefficients, W is the axle-load and ε and λ are geometrical parameters. If R is the radius of

curvature of the wheel tread and R' is that of the rail head then it is shown in [1] that

$$\varepsilon = l/(R-R') \tag{3}$$

and the effective conicity

$$\lambda = R\delta_0/(R-R'), \tag{4}$$

δ_0 being the slope of the contact plane when the wheelset is in the central position.

The following non-dimensional parameters, consistent with those used in [1], will be used in the analysis

$$\mu = 2fl/mV_0^2, \qquad \mu' = 2f'l/mV_0^2,$$

$$\alpha = \lambda l/r_0, \qquad v = V/V_0, \qquad s = \frac{l}{V_0}\frac{\mathrm{d}}{\mathrm{d}t},$$

$$j = C/ml^2, \qquad \rho = m'/m, \qquad \sigma = C'/ml^2,$$

$$\varepsilon_2 = 2k_2l^2/mV_0^2, \qquad \bar{\varepsilon}_2 = W\varepsilon l/mV_0^2, \qquad \bar{\bar{\varepsilon}}_2 = \varepsilon_2+\bar{\varepsilon}_2,$$

$$\psi_1 = q_1/l, \qquad \psi_2 = q_2, \qquad \psi_3 = q_3,$$

$$\psi_4 = q_4, \qquad \psi_5 = q_5/l, \qquad \psi_6 = q_6/l,$$

where V_0 is a reference velocity. The equations of motion then take the form

$$\begin{aligned}
\left(s^2+\frac{\mu'}{v}s+\bar{\bar{\varepsilon}}_2\right)\psi_1-\mu'\psi_2-h\varepsilon_2\psi_3 &= 0,\\
\mu\alpha\psi_1+\left(js^2+\frac{\mu}{v}s\right)\psi_2 &= 0,\\
-h\varepsilon_2\psi_1+(\tfrac{1}{2}\sigma s^2+h^2\varepsilon_2)\psi_3 &= 0,
\end{aligned} \tag{5}$$

and

$$\begin{aligned}
\left(s^2+\frac{\mu'}{v}s+\bar{\bar{\varepsilon}}_2\right)\psi_4-\mu'\psi_5-\varepsilon_2\psi_6 &= 0,\\
\mu\alpha\psi_4+\left(js^2+\frac{\mu}{v}s\right)\psi_5 &= 0,\\
-\varepsilon_2\psi_4+(\tfrac{1}{2}\rho s^2+\varepsilon_2)\psi_6 &= 0.
\end{aligned} \tag{6}$$

Both sets of equations are of exactly the same form. The equations of motion are unsymmetric due to the non-conservative nature of the forces due to the combined action of creep and conicity.

Some typical values (representative of British Rail practice) are

$r_0 = 1{\cdot}75$ ft,	$l = 2{\cdot}5$ ft,	$m = 90$ slugs,
$C = 360$ slugs ft^2,	$W = 9300$ lb,	$k_2 = 5000$ lb/ft,
$f = f' = 3\times10^6$ lbs,	$R' = 0{\cdot}690$ ft,	$R = 0{\cdot}787$ ft,
$\delta_0 = 0{\cdot}05$, $hl = 5$ ft,	$m' = 400$ slugs,	$C' = 12\times10^3$ slugs ft^2,

and taking the reference velocity $V_0 = 100$ ft/sec it follows that

$$\mu = \mu' = 16{\cdot}7, \qquad \alpha = 0{\cdot}571, \qquad j = 0{\cdot}640,$$
$$\varepsilon_2 = 0{\cdot}0694, \qquad \bar{\varepsilon}_2 = 0{\cdot}6562, \qquad h = 2{\cdot}00,$$
$$\sigma = 21{\cdot}3, \qquad \rho = 4{\cdot}44.$$

These numerical values will be used to illustrate the theory as it is developed.

On the assumption that the free motions of the system are of the type

$$q_r = K_r q^{\lambda t},$$

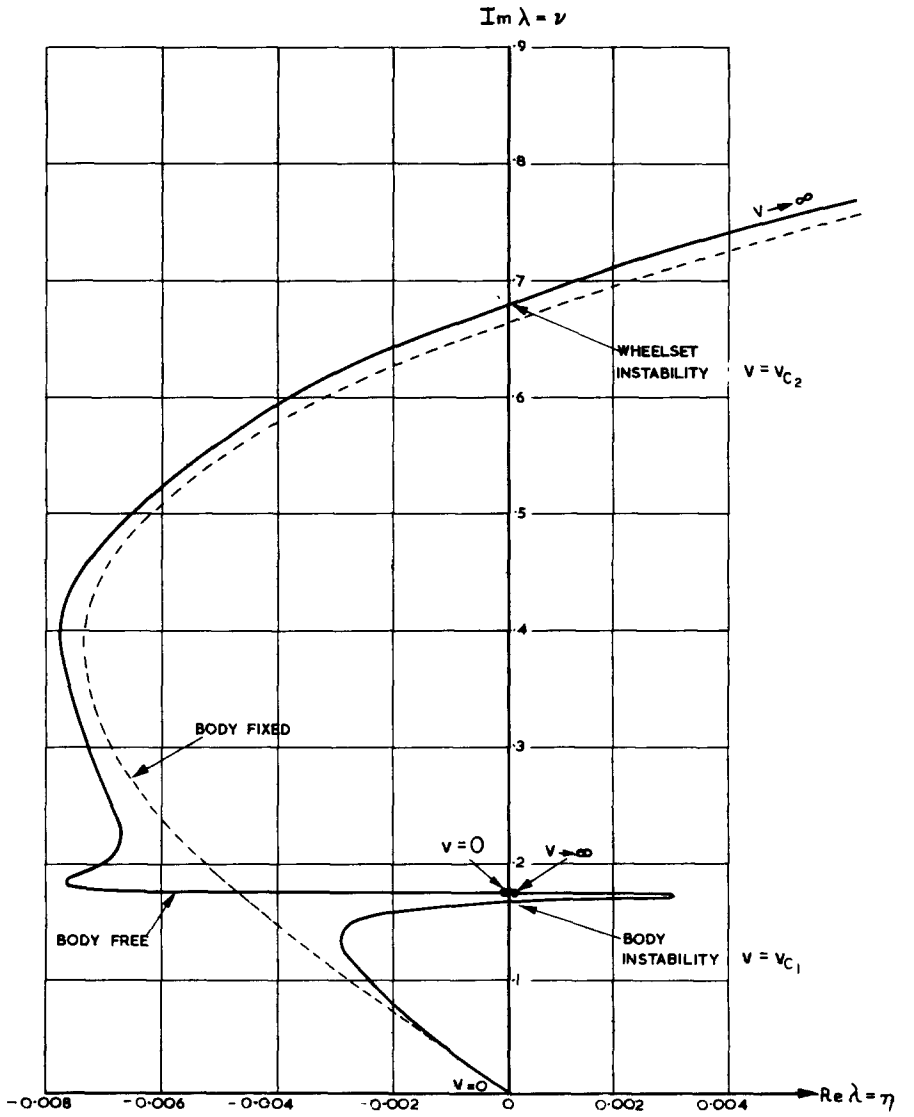

FIG. 3(a)

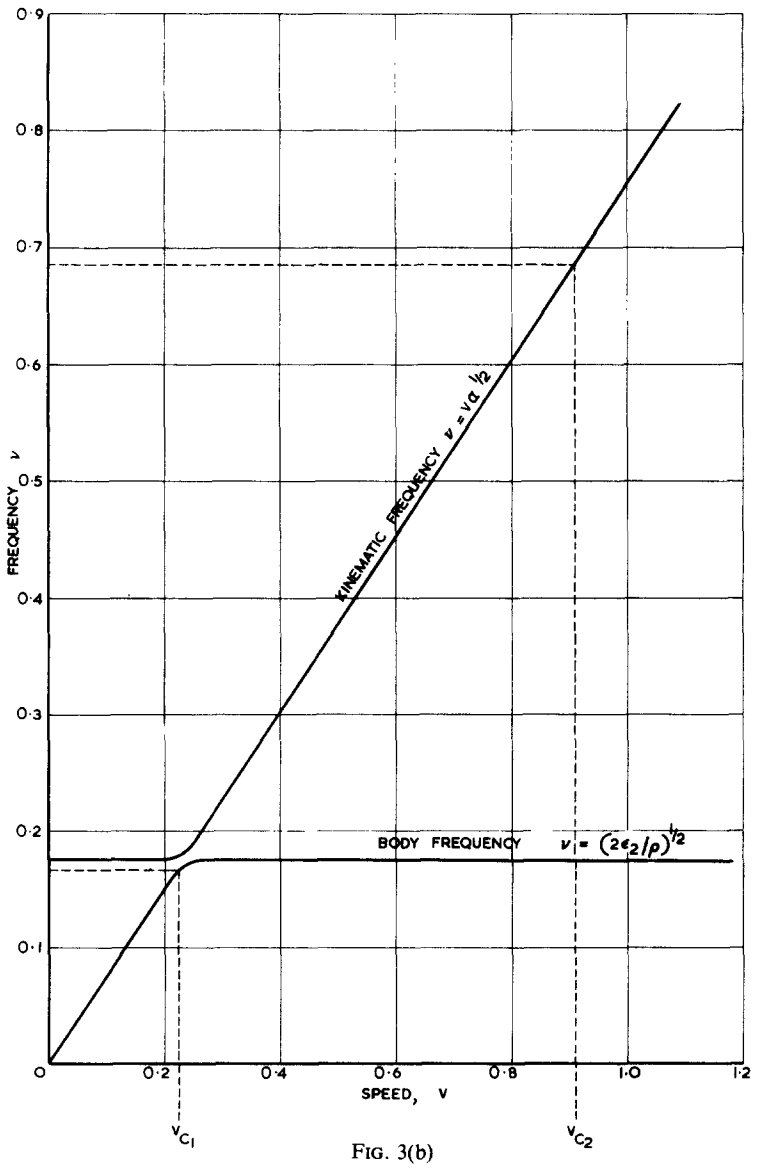

FIG. 3(b)

FIG. 3. Behaviour of roots of complete vehicle as speed is varied. (– – – root locus for elastically restrained wheelset.)

the equations of motion represented by equations (5) or (6) define an eigenvalue problem and typical solutions of this eigenvalue problem at various vehicle speeds are shown in Fig. 3, for the case where the suspension damping is zero. The figure shows only those solutions corresponding to oscillatory constituents; for there are two roots which are real, negative and have large values. These correspond to heavily damped subsidences involving either lateral translation or yaw of the wheelsets. Similar subsidences occurred in the case of the elastically restrained wheelset [1], and as this type of motion is heavily damped at all speeds it need not be considered any further. The remainder of the roots

correspond to oscillatory motions and are shown in Fig. 3(a). The variation of the frequency of each constituent with speed is shown in Fig. 3(b). At any given speed, there are two oscillatory constituents, one of which possesses a frequency which is very closely the same as the kinematic frequency associated with a wheelset, the other possessing a frequency which is very closely equal to the natural frequency of the vehicle body oscillating on the suspension with the wheels fixed.

The root locus in Fig. 3(a) indicates that at low speeds the damping in each mode is positive, for all the real parts of the roots are negative. As the speed is increased, the damping in each mode eventually becomes negative indicating instability. There is, therefore, for this particular example, a critical speed for each of the two oscillatory constituents. Corresponding to the body mode a critical speed occurs which is somewhat less than the speed at which frequency coincidence between the wheelset kinematic frequency and the natural frequency of the body mode occurs. The degree of instability, as measured by the maximum value of the real part of the root, in this case is limited. This instability will be termed body instability. At higher speeds, a further critical speed occurs, and comparison with the root locus of the system with body fixed, also shown in Fig. 3(a) shows that this is associated with the wheelset instability investigated in [1]. The accuracy with which the approximate root locus of the elastically restrained wheelset agrees with the root locus of the complete vehicle at the higher speeds justifies the approximation used in [1] of neglecting body motion. Above the critical speed corresponding to the wheelset instability, the real parts of the roots increase rapidly with increasing speed.

The numerical values shown in Fig. 3 correspond to the solution of equations (6), involving lateral translation of the body, for the example vehicle; similar characteristics would be obtained for equations (5) involving yaw of the body.

APPROXIMATE LOW SPEED ROOT LOCUS

At low speeds, the frequencies of the free motions of the vehicle are sufficiently low to justify neglecting the mass and moment of inertia in yaw of the wheelset, so that the equations of motion to be considered become

$$\left(\frac{\mu'}{v}s+\bar{\varepsilon}_2\right)\psi_4-\mu'\psi_5-\varepsilon_2\psi_6=0,$$

$$\mu\alpha\psi_4+\frac{\mu}{v}s\psi_5=0, \tag{7}$$

$$-\varepsilon_2\psi_4+(\tfrac{1}{2}\rho s^2+\varepsilon_2)\psi_6=0,$$

in the absence of suspension damping, the effect of which will be considered later. For a free motion of the type

$$q_r = K_r e^{\lambda t}$$

the characteristic equation of the system is

$$p_4\lambda^4+p_3\lambda^2+p_2\lambda^2+p_1\lambda+p_0=0, \tag{8}$$

where

$$p_4 = \rho/2\varepsilon_2, \qquad p_3 = \rho v\bar{\bar{\varepsilon}}_2/2\mu'\varepsilon_2,$$

$$p_2 = 1+\frac{\alpha\rho v^2}{2\varepsilon_2}, \qquad p_1 = v\bar{\varepsilon}_2/\mu', \qquad p_0 = \alpha v^2.$$

Typical solutions of this quartic equation shows that it possesses two pairs of conjugate complex roots; one pair with a large and the other with a small modulus. An approximation to the roots with large modulus is found by equating to zero the sum of the first three terms in the characteristic equation. An approximation to the roots with small modulus is found by ensuring that the product of the approximate quadratic factors yields the correct values for p_0 and p_1. In addition, since the speed is considered to be low, αv^2 may be neglected in comparison with $2\varepsilon_2/\rho$ so that the coefficient p_2 will be approximately unity. The characteristic equation then factorizes as

$$(\lambda^2+2\eta_1\lambda+\nu_1^2)(\lambda^2+2\eta_2\lambda+\nu_2^2) = 0, \tag{9}$$

where

$$\eta_1 = v\bar{\bar{\varepsilon}}_2/2\mu',$$

$$\nu_1^2 = 2\varepsilon_2/\rho,$$

$$\eta_2 = \frac{\bar{\varepsilon}_2 v}{2\mu'}\left[1-\frac{\alpha v^2\rho\bar{\bar{\varepsilon}}_2}{2\varepsilon_2\bar{\varepsilon}_2}\right],$$

$$\nu_2^2 = \alpha v^2.$$

The first oscillatory constituent, with roots $\eta_1 \pm i\nu_1$, has positive damping and the frequency corresponds to lateral oscillations of the body on the suspension. The second oscillatory constituent, with roots $\eta_2 \pm i\nu_2$, has the same frequency as the kinematic oscillation of a single wheelset [1]. The damping of this constituent vanishes at a critical speed v_c given by

$$v_c^2 = \frac{2\varepsilon_2\bar{\varepsilon}_2}{\alpha\rho\bar{\bar{\varepsilon}}_2}. \tag{10}$$

The critical speed is inversely proportional to the square root of the conicity and to the square root of the body mass. The frequency ν_c at which instability occurs, is given by

$$\nu_c^2 = \frac{2\varepsilon_2\bar{\varepsilon}_2}{\rho\bar{\bar{\varepsilon}}_2}. \tag{11}$$

Equation (10) indicates that the critical speed is zero when the gravitational stiffness $\bar{\varepsilon}_2$ is zero. As the gravitational stiffness is increased, the critical speed increases to a limiting value, given by

$$v_c^2 = \frac{2\varepsilon_2}{\rho\alpha}, \qquad \bar{\varepsilon}_2 \to \infty.$$

This is the speed for which frequency coincidence between the kinematical oscillation of a single wheelset and the natural mode of oscillation of the body on the suspension occurs. If the lateral suspension stiffness ε_2 is increased the critical speed is increased up to a limiting value given by

$$v_c^2 = \frac{2\bar{\varepsilon}_2}{\rho\alpha}, \qquad \varepsilon_2 \to \infty. \tag{12}$$

In this limiting condition, the body and the wheelsets move laterally without relative displacement.

The critical speed is, in the absence of suspension damping, independent of the values of the longitudinal and lateral creep coefficients. For the example vehicle, the critical speed of the instability involving lateral translation of the body is 22·3 ft/sec and the corresponding critical frequency is 1·07 c/s. The maximum damping factor (i.e. fraction of critical damping) occurs at low speeds and is

$$\left.\frac{\eta_2}{\nu_2}\right|_{v\to 0} = \varepsilon_2/2\mu'\sqrt{\alpha} \tag{13}$$

which amounts to only 0·0260 for the example vehicle. There is a corresponding analysis for the instability involving the yawing motions of the body, as governed by equations (5), and for the example vehicle the critical speed is 20·3 ft/sec and the critical frequency is 0·980 c/s.

STABILITY OF VEHICLE WITH SUSPENSION DAMPING AND ZERO WHEELSET INERTIA

The solution of equations (6) for the critical conditions for which sinusoidal oscillations of frequency ν are possible, will now be considered. The effect of wheelset mass and moment of inertia will be neglected, but suspension damping will be allowed for. The law representing the action of an actual damper element depends, of course, on the type of damper. In the present analysis it will be assumed that the hysteretic approximation is valid, so that the action of the suspension is described in terms of a complex mechanical impedance $\varepsilon_2(1+ig)$ where g is the hysteretic loss factor. This approximation has the advantage that the analysis is very much simpler than if the viscous damping approximation were taken. Since the remainder of the analysis is concerned with harmonic motion at a critical speed, the implications of the dependence of ε_2 and g upon frequency which may arise in the case of actual suspension elements may be readily assessed in practical applications of the theory, but it is assumed here that ε_2 and g are independent of frequency. Accordingly, the stability determinant becomes

$$\begin{vmatrix} \frac{\mu'}{v}i\nu+\delta_2+\varepsilon_2(1+ig) & -\mu' & -\varepsilon_2(1+ig) \\ \mu\alpha & \frac{\mu}{v}i\nu & 0 \\ -\varepsilon_2(1+ig) & 0 & -\frac{1}{2}\rho v^2+\varepsilon_2(1+ig) \end{vmatrix} = 0. \tag{14}$$

Equation (14) will be satisfied by the critical values of ν and v. On expansion, equation (14) becomes

$$\frac{\mu'}{v}i\nu+\delta_2-\frac{i\mu' v\alpha}{\nu} = \frac{1}{2}\rho v^2\left\{1+\frac{\frac{1}{2}\rho v^2}{[-\frac{1}{2}\rho v^2+\varepsilon_2(1+ig)]}\right\}. \tag{15}$$

The physical significance of equation (15) is that the L.H.S. represents the mechanical

impedance of the wheel/rail sub-system and the R.H.S. represents the mechanical impedance of the body and suspension sub-system. Separating real and imaginary parts,

$$\bar{\varepsilon}_2 = \frac{1}{2}\rho v^2\left[1+\frac{\frac{1}{2}\rho v^2(\varepsilon_2-\frac{1}{2}\rho v^2)}{(\varepsilon_2-\frac{1}{2}\rho v^2)^2+g^2\varepsilon_2^2}\right]$$

and

$$-\mu'+\frac{v^2\mu'\alpha}{v^2} = \frac{\frac{1}{4}\rho^2 v^3 g v\varepsilon_2}{(\varepsilon_2-\frac{1}{2}\rho v^2)^2+g^2\varepsilon_2^2},$$

or defining

$$\Omega^2 = v^2\rho/2\varepsilon_2, \qquad \Lambda = v/v, \qquad G = \varepsilon_2 g/\mu'\alpha,$$

these equations become

$$\frac{\bar{\varepsilon}_2}{\varepsilon_2} = \Omega^2\left[1+\frac{\Omega^2(1-\Omega^2)}{(1-\Omega^2)^2+g^2}\right], \tag{16}$$

$$\Lambda^2-\left[\frac{G\Omega^4}{(1-\Omega^2)^2+g^2}\right]\Lambda-\frac{1}{\alpha} = 0. \tag{17}$$

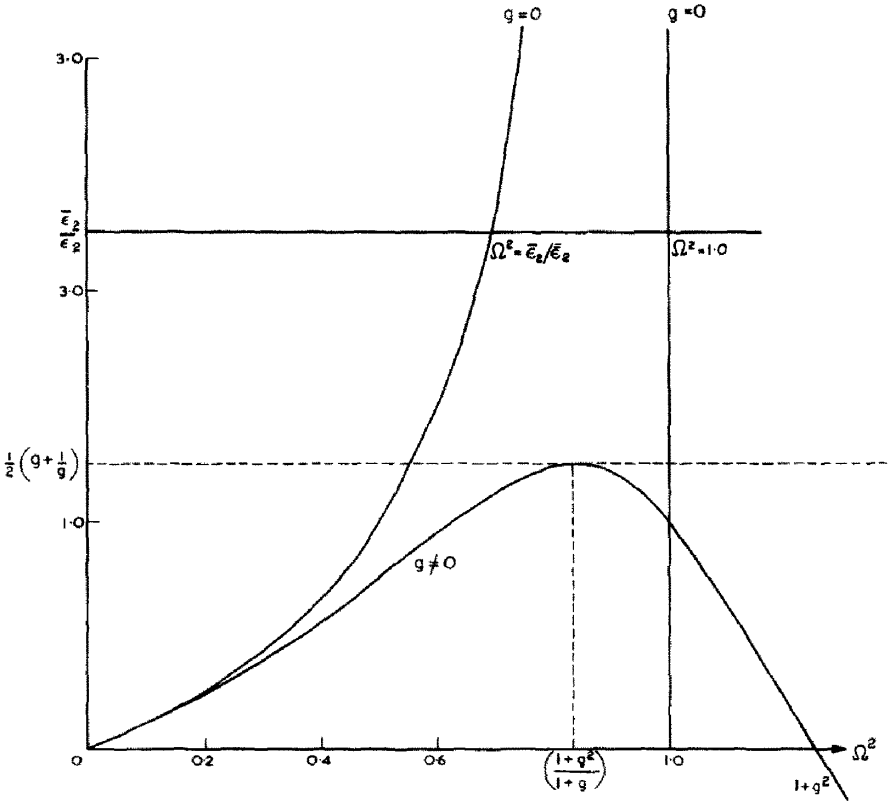

FIG. 4. Determination of critical frequencies.

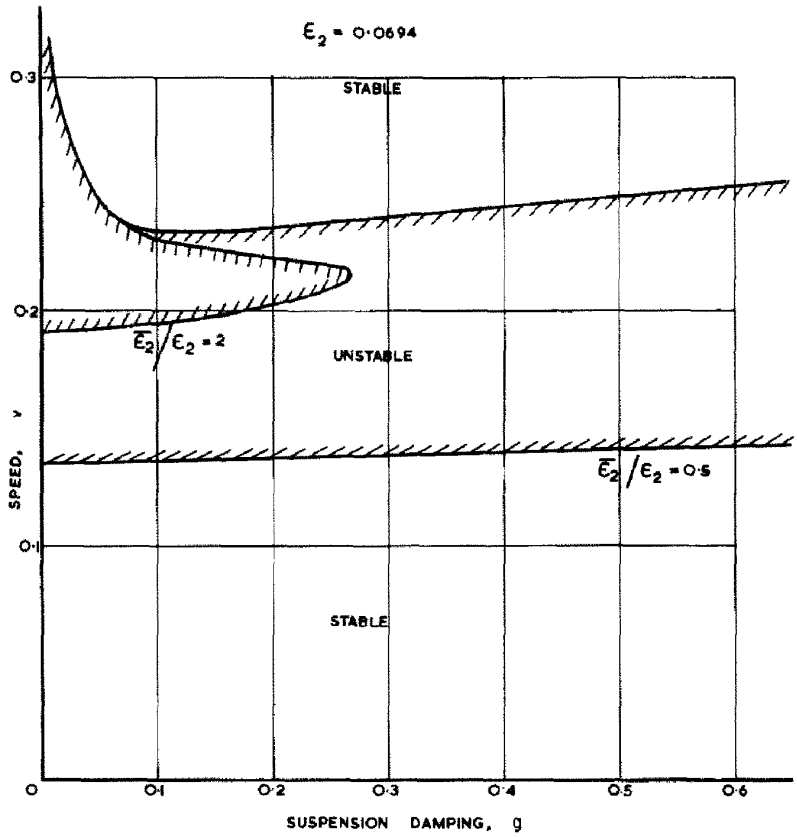

FIG. 5. Effect of suspension damping on stability.

Equation (16) yields the critical frequencies Ω_c which depend only on the ratio $\bar{\varepsilon}_2/\varepsilon_2$ and g. Equation (17) then yields the corresponding critical wavelengths Λ_c and hence the critical speeds. Figure 5 shows the L.H.S. and R.H.S. of equation (16) each plotted against frequency squared Ω^2. The critical frequencies are given by the intersections of the two curves, and can be determined by solving the quadratic

$$\left(1+\frac{\bar{\varepsilon}_2}{\varepsilon_2}\right)\Omega^4-\left(1+2\frac{\bar{\varepsilon}_2}{\varepsilon_2}+g^2\right)\Omega^2+\frac{\bar{\varepsilon}_2}{\varepsilon_2}(1+g^2)=0 \tag{18}$$

which is equivalent to equation (16). As indicated by Fig. 4 the upper critical frequency Ω^2 is always less in value than $(1+g^2)$ and consequently equation (17) yields only one critical wavelength Λ_c corresponding to each critical frequency.

For the case of zero suspension damping, $g = 0$ equation (18) yields two solutions which are

$$\Omega_c^2 = \bar{\varepsilon}_2/\varepsilon_2, \qquad \Omega_c^2 = 1,$$

corresponding to

$$v^2 = 2\varepsilon_2\bar{\varepsilon}_2/\rho\bar{\varepsilon}_2, \qquad v^2 = 2\varepsilon_2/\rho.$$

The corresponding critical speeds are obtained from equation (17)

$$\Lambda^2 = 1/\alpha, \qquad \Lambda = \infty,$$

so that

$$v^2 = 2\varepsilon_2\bar{\varepsilon}_2/\rho\alpha\bar{\varepsilon}_2, \qquad v = \infty.$$

These results are, of course, in exact agreement with those obtained by the approximate factorization of the characteristic equation. The system is unstable at all speeds above the lower critical speed.

For the system with suspension damping Fig. 4 indicates that for small values of the ratio $\bar{\varepsilon}_2/\varepsilon_2$ there are two critical frequencies, as in the case of zero suspension damping. At a particular value of the ratio $\bar{\varepsilon}_2/\varepsilon_2$ only one critical frequency occurs, and for larger values of the ratio there will be stability at all speeds. The condition for equation (18) to have only one real solution is

$$\left(1+\frac{2\bar{\varepsilon}_2}{\varepsilon_2}+g^2\right)^2 = 4\left(1+\frac{\bar{\varepsilon}_2}{\varepsilon_2}\right)(1+g^2)\frac{\bar{\varepsilon}_2}{\varepsilon_2}$$

which reduces to

$$\frac{\bar{\varepsilon}_2}{\varepsilon_2} = \frac{1}{2}\left(g+\frac{1}{g}\right). \tag{19}$$

The corresponding critical frequency is

$$\Omega^2 = (1+g^2)/(1+g). \tag{20}$$

If

$$\frac{\bar{\varepsilon}_2}{\varepsilon_2} > \frac{1}{2}\left(g+\frac{1}{g}\right), \tag{21}$$

stability exists at all speeds. Since the minimum value of the R.H.S. of the inequality (21) is unity a necessary condition for stability at all speeds is simply

$$\bar{\varepsilon}_2 > \varepsilon_2.$$

If this condition is not satisfied, instability cannot be prevented by the provision of suspension damping. Equation (21) also implies that, in order to obtain stability at all speeds for a given value of the ratio $\bar{\varepsilon}_2/\varepsilon_2$ it is necessary for the suspension damping to take a value between certain limits. Instability will occur at some speed if the suspension damping is either too small or too large. The effect of suspension damping on the critical speeds in two cases $\bar{\varepsilon}_2/\varepsilon_2 = 0{\cdot}5$ and $\bar{\varepsilon}_2/\varepsilon_2 = 2$, shown in Fig. 5.

The motion of the vehicle, in the critical mode and at a critical speed will take the form

$$\begin{aligned} \psi_4 &= -a_4 \cos \nu_c t, \\ \psi_5 &= a_5 \sin \nu_c t, \\ \psi_6 &= -a_6 \cos(\nu_c t+\theta), \end{aligned} \tag{22}$$

so that θ is the phase angle between lateral translation of the wheelset and lateral translation of the body. Since

$$\mu\alpha\psi_4+\frac{\mu}{v}s\psi_5 = 0,$$
$$-\varepsilon_2(1+ig)\psi_4+[\tfrac{1}{2}\rho s^2+\varepsilon_2(1+ig)]\psi_6 = 0, \tag{23}$$

the relative amplitudes are

$$\left(\frac{a_5}{a_4}\right)^2 = \alpha^2v^2/v^2,$$
$$\left(\frac{a_6}{a_4}\right)^2 = (1+g^2)/[(1-\Omega^2)^2+g^2], \tag{24}$$

and the phase angle is given by

$$\tan\theta = \Omega^2g/(1-\Omega^2+g^2), \tag{25}$$

the motion of the wheelsets is, therefore, identical to that in the kinematic mode of an isolated wheelset [1] in the case where the suspension damping is zero; the amplitude ratio (a_6/a_4) reduces to $\bar{\varepsilon}_2/\varepsilon_2$ and the corresponding phase angle is zero so that the lateral displacement of the body is in phase with the lateral displacement of the wheelset. The

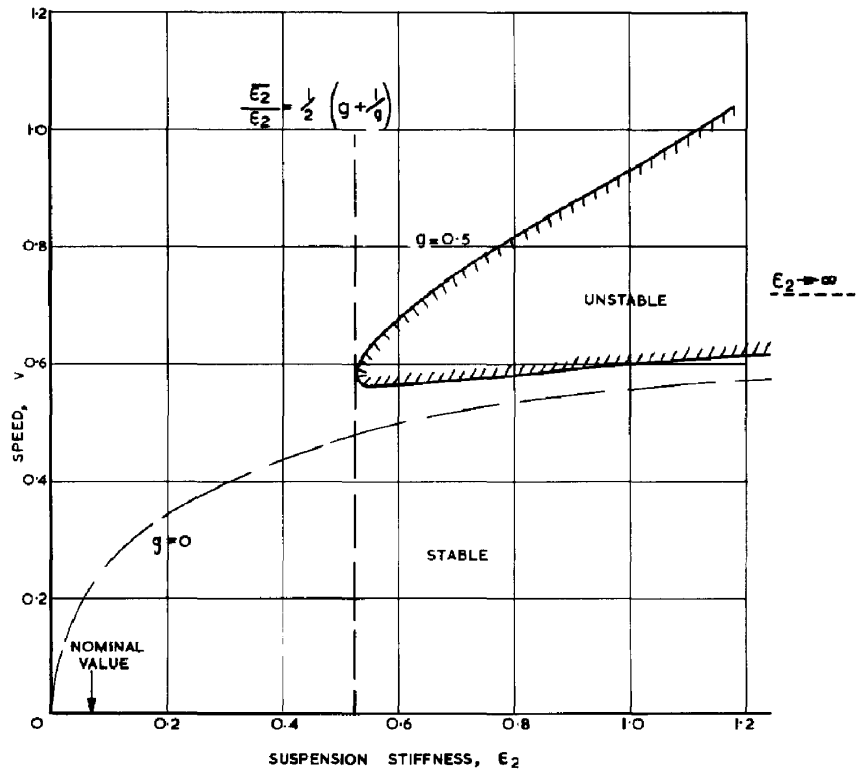

FIG. 6. Stability as a function of suspension stiffness and speed.

amplitude ratio increases with increasing gravitational stiffness, so that whereas the amplitude ratio is unity in the case of coned wheels, it amounts to 10·5 in the case of the example vehicle with profiled wheels.

Figure 6 shows the stability boundary as a function of forward speed v and suspension stiffness ε_2 for the example vehicle, in the case where the suspension damping $g = 0{\cdot}5$. For small values of suspension stiffness there is stability at all speeds. For large values of the suspension stiffness there are two critical speeds and a region of instability. For comparative purposes, the stability boundary for the same system, but with zero suspension damping, is shown by the broken line in Fig. 6. As shown above the lower critical speed is raised by increasing suspension stiffness until a limiting value is reached which is given by equation (12), which is 72 ft/sec for the example vehicle.

As discussed in [1], wheels which initially possess conical treads are rapidly worn so that the treads become concave. During the wearing process, the slope of the contact plane δ_0 remains constant, but the radius of curvature of the wheel tread decreases rapidly until a profile is obtained which is not subject to any further change. For the numerical example given above, reduction in the radius of curvature of the wheel tread R increases the effective conicity λ, given by equation (4), from 0·05 (the value of δ_0) when the radius is

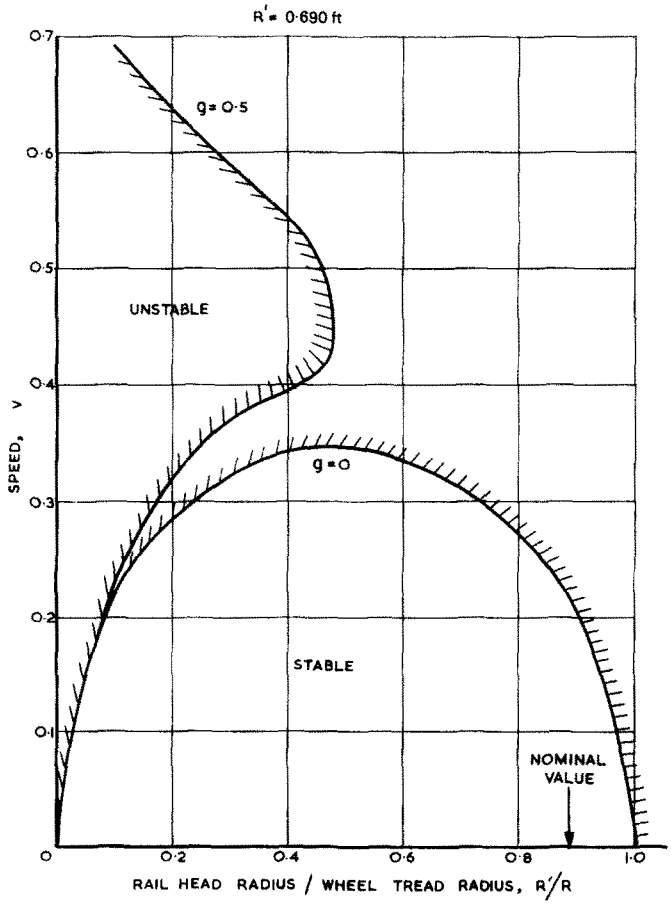

FIG. 7. Effect of wheel and rail curvature on stability.

infinite to 0·40 when the radius is 0·787 ft; the latter corresponds to a profile of a fully worn wheel, and the rail head radius R' is, as specified above, 0·690 ft. The variation of critical speed for the example vehicle, for $g = 0$ and $g = 0{\cdot}5$, is shown in Fig. 7. Increasing the ratio R'/R, increases the gravitational stiffness and consequently if there is suspension damping a point will be reached where the vehicle is stable at all speeds. Increasing the ratio R'/R also increases the effective conicity which tends to reduce the critical speed as indicated by equation (17).

THE EFFECT OF WHEELSET INERTIA ON STABILITY

In the previous analysis of stability, wheelset mass and moment of inertia was neglected. The treatment of stability can be extended to include the effect of wheelset inertia, and assuming as before that the suspension damping can be described by the hysteretic approximation, this requires the consideration of the stability determinant in the form

$$\begin{vmatrix} -\nu^2+\frac{\mu'}{v}i\nu+\bar{\varepsilon}_2+\varepsilon_2(1+ig) & -\mu' & -\varepsilon_2(1+ig) \\ \mu\alpha & -j\nu^2+\frac{\mu}{v}i\nu & 0 \\ -\varepsilon_2(1+ig) & 0 & -\frac{1}{2}\rho v^2+\varepsilon_2(1+ig) \end{vmatrix} = 0 \qquad (26)$$

where ν is the frequency of the oscillation at a critical speed. On expansion and separation of real and imaginary parts, equation (26) becomes

$$-\nu^2+\bar{\varepsilon}_2-\frac{\mu\mu'\alpha j}{[j\nu^2+(\mu^2/v^2)]} = \frac{1}{2}\rho v^2\left\{1+\frac{\frac{1}{2}\rho v^2(\varepsilon_2-\frac{1}{2}\rho v^2)}{[(\varepsilon_2-\frac{1}{2}\rho v^2)^2+g^2\varepsilon_2^2]}\right\} \qquad (27)$$

and

$$-\frac{\mu'}{v}+\frac{\mu'\mu^2}{v\nu^2[j^2\nu^2+(\mu^2/v^2)]} = \frac{\frac{1}{4}\rho^2\nu^3\varepsilon_2 g}{[(\varepsilon_2-\frac{1}{2}\rho v^2)^2+g^2\varepsilon_2^2]}. \qquad (28)$$

As before, these expressions represent the equality of the mechanical impedance of the wheel/rail sub-system (on the L.H.S.) and the mechanical impedance of the body and suspension sub-system (on the R.H.S.) at the critical condition. The inclusion of wheelset inertia has merely altered the L.H.S. of these equations. Now, in practical cases, the creep coefficients are large compared with the inertia coefficients so that it is reasonable to neglect $j^2\nu^2$ compared with μ^2/v^2 in equation (28). Introducing the quantities Ω^2, Λ and G defined above, equation (28) then reduces to equation (17). With this approximation, the relationship between critical frequency and critical speed is not affected by the introduction of wheelset inertia. In accordance with the same approximation equation (27) becomes

$$\bar{\varepsilon}_2-\nu^2-\frac{\mu'}{\mu}j\alpha v^2 = \frac{1}{2}\rho v^2\left\{1+\frac{\frac{1}{2}\rho v^2(\varepsilon_2-\frac{1}{2}\rho v^2)}{[(\varepsilon_2-\frac{1}{2}\rho v^2)^2+g^2\varepsilon_2^2]}\right\}. \qquad (29)$$

An approximate solution of equations (27) and (28) may be obtained by noting that the lower critical speed of the body instability and the critical speed of the wheelset instability occur at the kinematic wavelength so that

$$\Lambda^2 = 1/\alpha, \qquad \text{i.e. } v^2 = \alpha v^2,$$

so that equation (29) may be written as

$$\frac{\bar{\varepsilon}_2}{\varepsilon_2} - \Omega^2\left(\frac{2\mu + 2\mu' j}{\mu\rho}\right) = \Omega^2\left[1 + \frac{\Omega^2(1-\Omega^2)}{(1-\Omega^2)^2 + g^2}\right]. \tag{30}$$

The ratio $(2\mu + 2\mu' j)/\mu\rho$ represents the ratio of the effective inertia of the wheelset to half the body mass. Equation (30) determines the critical frequencies of the system, and hence the critical speeds.

In the case of zero suspension damping, there are two critical frequencies, given by the solutions of the quadratic in Ω^2.

$$K\Omega^4 - \left(1 + \frac{\bar{\varepsilon}_2}{\varepsilon_2} + K\right)\Omega^2 + \frac{\bar{\varepsilon}_2}{\varepsilon_2} = 0$$

where

$$K = (2\mu + 2\mu' j)/\rho\mu.$$

One solution occurs at relatively low frequencies and can, therefore, be approximated by

$$\Omega^2 = \frac{\bar{\varepsilon}_2}{\varepsilon_2} \Big/ \left(1 + \frac{\bar{\varepsilon}_2}{\varepsilon_2} + K\right)$$

reducing to

$$v^2 = 2\bar{\varepsilon}_2\varepsilon_2 \Big/ \left(\rho\bar{\varepsilon}_2 + 2\varepsilon_2 + 2\varepsilon_2 \frac{\mu'}{\mu} j\right).$$

The corresponding critical speed is

$$v^2 = 2\bar{\varepsilon}_2\varepsilon_2/\alpha\left(\rho\bar{\varepsilon}_2 + 2\varepsilon_2 + 2\varepsilon_2 \frac{\mu'}{\mu} j\right). \tag{31}$$

This shows that including the wheelset mass and moment of inertia reduces the critical speed associated with the instability of the body. The reduction is a maximum when the gravitational stiffness is small, and in the case of the example vehicle the critical speed is reduced from 22·3 ft/sec to 21·0 ft/sec. The other solution occurs at high frequencies, and can be approximated by

$$\Omega^2 = \left(1 + \frac{\bar{\varepsilon}_2}{\varepsilon_2} + K\right)/K$$

which is equivalent to

$$v^2 = \frac{\bar{\varepsilon}_2\mu}{\alpha(\mu + \mu' j)} + \frac{2\varepsilon_2}{\rho\alpha}. \tag{32}$$

This critical speed is associated with instability of a wheelset which has been discussed in [1]. If the body mass is assumed to be very large then

$$v^2 = \bar{\varepsilon}_2\mu/\alpha(\mu + \mu' j)$$

which, in the absence of longitudinal suspension stiffness, is equation (14) of [1]. Allowance for body motion, therefore, increases the critical speed, and in the case of the example vehicle the critical speed is increased from 88 ft/sec to 91 ft/sec.

The vehicle is unstable at all speeds above the lower critical speed in the absence of suspension damping, as indicated by Fig. 3 which shows the behaviour of the oscillatory roots of the characteristic equation as the speed is varied.

In the case where the vehicle has suspension damping, then for negligible wheelset inertia the condition for stability at all speeds is expressed by the inequality (21). If the wheelset inertia is not neglected, a critical speed associated with instability of the wheelset occurs. This critical speed is less than the critical speed given by equation (32), the reduction in critical speed being due to the introduction of suspension damping. As the wheelset inertia is increased, the critical speed is reduced. As indicated by Fig. 8, for values of wheelset inertia greater than a certain value, three critical speeds occur. As before, the upper critical speed refers to the wheelset instability, and the lower critical speeds enclose a range of speeds for which the body instability occurs. For sufficiently

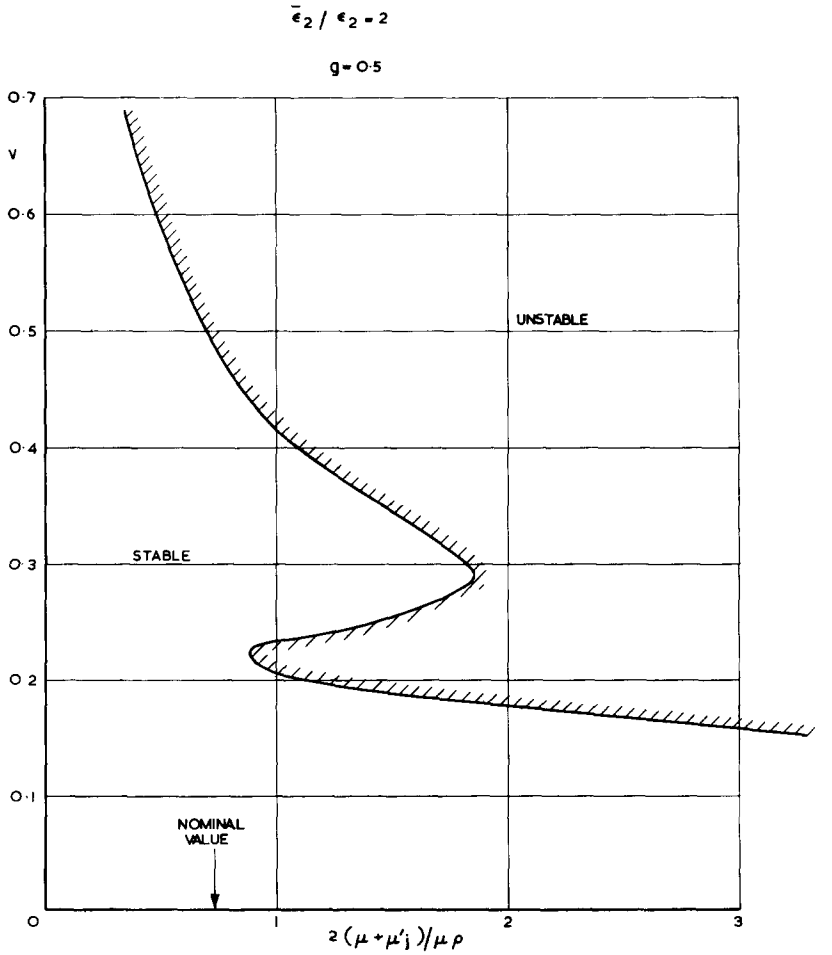

FIG. 8. Effect of wheelset inertia on stability.

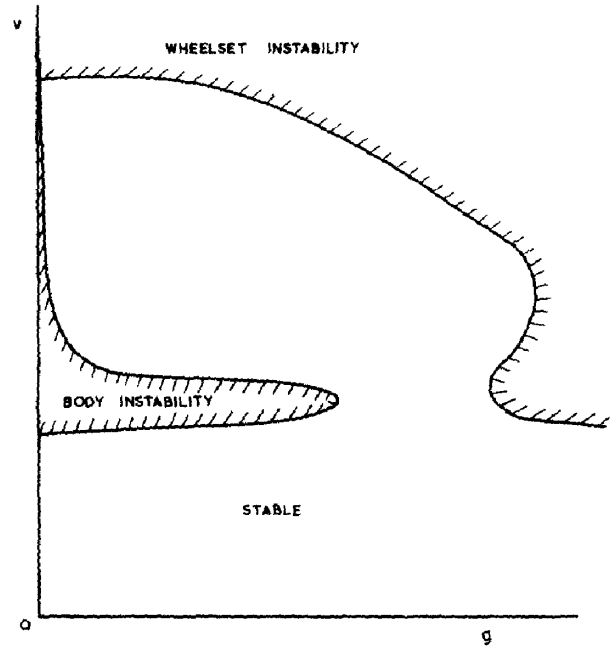

(a) $\bar{\epsilon}_2 \gg \epsilon_2$

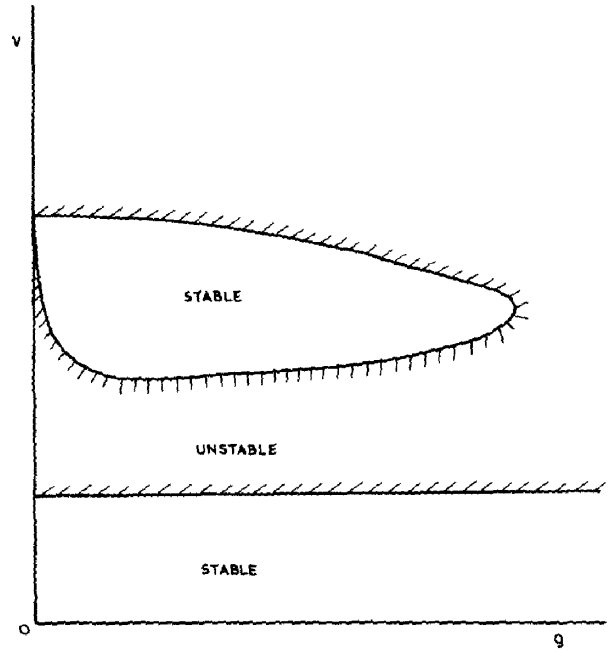

(b) $\bar{\epsilon}_2 \ll \epsilon_2$

FIG. 9. Effect of damping on stability for small and large gravitational stiffnesses.

large values of wheelset inertia, the regions of wheelset instability and body instability merge, and there is only one critical speed. This critical speed corresponds to that given by equation (31) in the case of zero suspension damping. The effect of suspension damping is always to increase this lower critical speed.

For a given wheelset inertia, the effect of suspension damping and gravitational stiffness on stability is indicated by Fig. 9. If the gravitational stiffness $\bar{\varepsilon}_2$ is sufficiently larger than the suspension stiffness ε_2, there is a range of suspension damping g for which body instability does not occur. Increasing the suspension damping also reduces the critical speed of the wheelset instability, so that for larger values of suspension damping, the regions in the stability diagram shown in Fig. 9 corresponding to body instability and wheelset instability coalesce. However, if $\bar{\varepsilon}_2$ is rather smaller than ε_2, increasing the suspension damping does not eliminate the body instability, but the critical speed of the wheelset instability is reduced as before so that for larger values of suspension damping the regions corresponding to body instability and wheelset instability again coalesce.

In the absence of suspension damping, as the lateral suspension stiffness is increased the critical speed increases to a limiting value given by

$$v_c^2 = \mu\bar{\varepsilon}_2/\alpha\left[j\mu' + \left(1+\frac{\rho}{2}\right)\mu\right] \tag{33}$$

which reduces to equation (12) if wheelset inertia is neglected.

APPLICATION OF THE THEORY

It has been shown that a railway vehicle of the type considered here may experience dynamic instability of two kinds; the first kind of instability, investigated in the present paper, has been termed body instability and can occur at relatively low speeds. The second kind of instability is termed wheelset instability and was investigated in [1]. For the complete vehicle, there are two possible modes of body instability, one associated with the lateral translation of the vehicle body and the other associated with the yawing motion of the body. In addition, there are two possible modes of wheelset instability, one of which involves both wheelsets moving in phase and the other involving the wheelsets moving in antiphase. Figure 10 indicates the variation of the four critical speeds with lateral suspension stiffness in a typical case. For given values of the gravitational stiffness $\bar{\varepsilon}_2$ and suspension damping g, it can be seen that for small values of the lateral suspension stiffness, the critical speed is that associated with the wheelset instability. For large values of suspension stiffness, the critical speed is that corresponding to the body instability. For certain intermediate values of suspension stiffness, there is a range of speeds above the speeds at which the body instability occurs, for which the system is stable, but this cannot be exploited in practice. These results indicate two possibilities for the rational design of a railway vehicle for stable running. The first is to use a relatively stiff suspension, so that the operating speed of the vehicle is limited by the occurrence of the body instability and the second is to use a relatively flexible, damped suspension so that the operating speed of the vehicle is limited by the occurrence of the wheelset instability.

If the design employs a stiff suspension, suspension damping will not have a large effect on the critical speed which will then be given by equation (31). The mass and moment of inertia of the wheelset should be kept to a minimum, and the lateral suspension

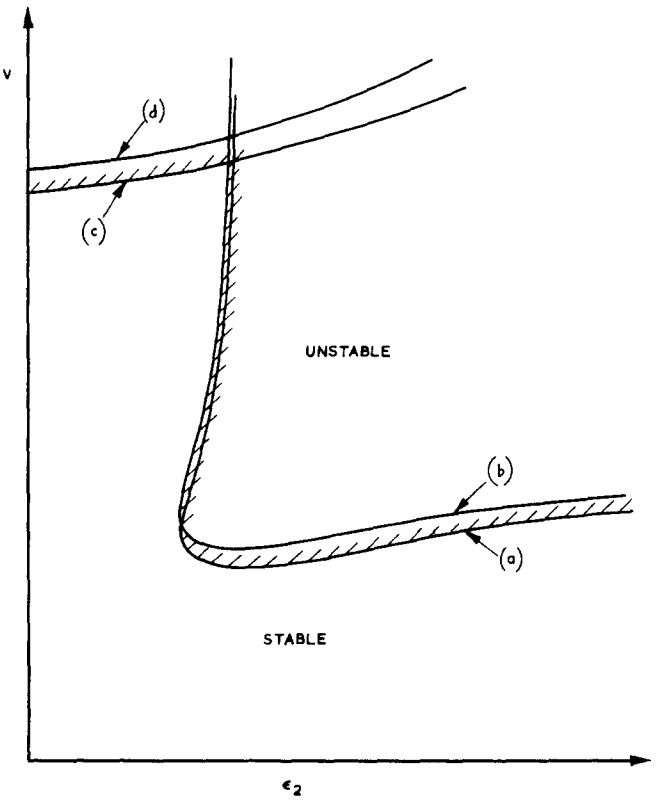

FIG. 10. Stability of complete vehicle as a function of speed and lateral suspension stiffness: (a) critical speed associated with body lateral translation, (b) critical speed associated with body yaw, (c) wheelsets in phase, (d) wheelsets in antiphase.

stiffness should be as large as possible consistent with other design requirements. If the vehicle body is rigidly connected with the wheelsets in the lateral direction, a maximum value of the critical speed will be obtained, which is given by equation (33). The gravitational stiffness $\bar{\epsilon}_2$ should be large and the effective conicity α small for stability. Considerations of static stability limits the reduction of the effective conicity, which could, in principle, be varied independently of the curvatures of rail and wheel by variation of the angle of the tread δ_0 (see equation (4)). Similarly, as the ratio of the radius of curvature of the rail head R' to the radius of curvature of the wheel tread R is varied, a maximum value for the critical speed is obtained, so that an optimum value of R'/R exists, giving the optimum combination of gravitational stiffness $\bar{\epsilon}_2$ and effective conicity α. However, it is doubtful whether variations in R, R' and δ_0 can be exploited, as the values of R, R' and δ_0 depend on wear. It is known that the treads of wheels wear rapidly until a profile is obtained which is not subject to any further change, and it is suggested that the vehicle should be designed so that satisfactory behaviour is obtained with wheels which possess profiles approximating to the fully worn profile. This has the advantage that no variations in the parameters of the system should be caused by further wear. The gravitational stiffness is proportional to axle-load and it follows that increasing the axle-load is stabilizing. The influence of realistic variations in the values of the creep coefficients is small.

As mentioned previously, the lowest critical speed for the example vehicle, which has a rather flexible suspension, is 20·3 ft/sec. Employing a stiff suspension, as discussed here, would raise this critical speed up to a maximum of 51·7 ft/sec, according to equation (33).

Design employing a damped, flexible suspension depends on the elimination of the body instability and the raising of the critical speed of the wheelset instability as high as possible. The body instability can be eliminated by satisfying the inequality (21) which determines the relationship between the gravitational stiffness ε_2, the suspension stiffness ε_2 and the suspension damping g. The gravitational stiffness ε_2 should be large, and, therefore, profiled wheels are necessary. For the reasons discussed above, it is unlikely that variations in the curvatures of wheel and rail, and in the slope of the wheel tread δ_0 can be exploited in practice, and consequently wheels with profiles approximating to the worn profile are necessary. Since the critical speed of the wheelset instability, given by equation (32), increases with increasing suspension and gravitational stiffness, the suspension stiffness should be as large as possible, consistent with satisfying the inequality (21), and this requires a suitable value for the suspension damping. However, very large values of suspension damping will lead to unacceptable reductions in the critical speed corresponding to the wheelset instability, as shown in Fig. 9, so that an appropriate choice of suspension stiffness and damping is necessary. Wheelset mass and moment of inertia must be reduced as far as possible. For the example vehicle $\varepsilon_2/\varepsilon_2 = 9{\cdot}46$ so that the minimum damping required follows from the inequality (21) as $g = 0{\cdot}053$. The critical speed of wheelset instability is, from equation (32), 90·6 ft/sec, which represents a substantial increase over that obtained by using a stiff suspension.

Acknowledgements—Acknowledgement is made to Dr. S. Jones, Chief of Research, British Rail Board, for permission to publish this paper. I am grateful to Dr. D. Williams for many helpful comments during the preparation of this paper, and to P. J. Coates and his staff for the numerical solution of the eigenvalue problem shown in Fig. 3.

REFERENCES

[1] A. H. WICKENS, *Int. J. Solids Structures* **1**, 319–341 (1965).
[2] T. MATSUDEIRA, Paper awarded prize in the competition sponsored by Office of Research and Experiment of the International Union of Railways. Utrecht (1960).
[3] N. A. KOVALEV, *The lateral oscillations of rolling stock*. Transzheldorizdat, Moscow (1957).

(*Received* 28 *December* 1964)

Résumé—L'instabilité dynamique d'un véhicule de chemin de fer à quatre roues, provenant de l'action combinée des forces transversales entre les roues et les rails et de la conicité des roues, est étudiée par l'auteur pour le cas où le corps du véhicule est relié aux roues par l'intermédiaire d'une suspension élastique. L'auteur suppose que la rigidité de la suspension est négligeable dans le sens longitudinal et que la surface portante des roues est profilée au lieu d'être simplement conique. L'auteur montre qu'il existe deux possibilités d'instabilité; l'instabilité de la portance des roues qui se manifeste aux grandes vitesses et dans laquelle intervient principalement le mouvement des roues et l'instabilité du corps du véhicule qui apparait aux faibles vitesses et qui provoque de grands déplacements du corps. L'auteur démontre que la force de rappel provenant de la composante latérale de la réaction normale entre rous et rail, au cours d'un déplacement latéral, a une grande influence sur la stabilité et il montre comment cette influence peut être utilisée, en liaison avec l'amortissement de la suspension, pour faire l'étude correcte d'un véhicule de chemin de fer, stable aux grandes vitesses.

Абстракт—Динамическая неустойчивость четырехколесного железнодорожного вагона, обусловленная совместным действием сил ползучести, действующих между колесами и рельсами, и коничности колес, исследуется в том случае, когда корпус вагона присоединяется к колесам посредством упругой подвески. Подвеска рас читывается с тем, чтобы иметь незначительную жесткость в продольном направлении, и поверхность катания колес профилируется вместо того, чтобы быть чисто конической. Показывается, что существует два возможных типа неустойчивости: неустойчивость тележки, которая встречается при высоких скоростях и которая включает в себя главным образом перемещение тележки; и корпусная неустойчивость, которая имеет место при низких скоростях и включает в себя перемещение корпуса. Влияние восстанавливающей силы, которая является результатом поперечной составляющей изменения нормальной реакции между колесом и рельсом и поперечным перемещением, на устойчивость имеет большое значение; определяется, как это влияние может быть использовано в сочетании с в правильно спроектированных железнодорожных вагонах для ровного хода при высоких скоростях.